

# Experimental and Finite Element Investigation of Roll Drawing Process

F. Lambiase and A. Di Ilio

(Submitted July 8, 2010; in revised form February 2, 2011)

**In this research, the wire drawing process with flat roller dies is investigated. A prototypal apparatus is developed to conduct experimental tests on such a process and analyze the influence of main roll drawing parameters (e.g., incoming wire diameter, forming rolls diameter, thickness reduction, and friction conditions) on geometrical characteristics of flattened wires. A finite element model (FEM) is developed to simulate the deformation of the wire during the process. Within the entire range of experiments, a good agreement between experimental data and numerical results is found which allows validating the FE model. A further observation from the experimental program and numerical simulations is that a complicated dependence of the lateral spread of wire and width of contact area on process parameters exists during wire drawing with roller dies.**

**Keywords** finite element model, flat wires, geometrical characterization, roll drawing

## 1. Introduction

Flat wires are nowadays employed for different purposes; indeed, they are used as semi-finished products for later production of round wires, steel strips, springs other than finished products, i.e., cable connection, transformers, or in HI-FI applications. Flat wires are traditionally produced at room temperature by flat rolling process by rolling the wire in one or several passes (Ref 1, 2). The manufacturing of sound product with homogeneous mechanical, physical, and metallurgical properties depends on the correct design of wire flattening process. An improper design would result in an undesirable spread in wire leading to an unsatisfactory product (Ref 3).

In the recent years, a renewed interest toward such a process has aimed several authors to a better understanding of such a process. Several empirical, analytical, and numerical models have been proposed to forecast the final geometry of wire, the stress and strain distribution. Kazeminezhad and Karimi Taheri (Ref 4, 5) performed an experimental campaign on flat rolling process to analyze the strain inhomogeneity due to different reductions in height. Subsequently, they performed a comparison between the geometrical characteristics of wires produced with 3D flat rolling and 2D side-pressing processes. Vallelano et al. (Ref 6) developed a finite element model (FEM) to analyze the inhomogeneity of wires, the contact pressure, and residual stresses for different rolling reductions.

Nevertheless, flat wires can be also produced with drawing process by employing a couple of idle rolls rather than

motorized ones and applying a drawing force in longitudinal direction. The employment of roller dies, instead of a fixed one, has been studied in the past with the aim of reducing the flow stress and frictional forces in traditional drawing process.

Mechanical characteristics, i.e., structure, texture, residual stresses, surface roughness, etc. of round wires produced with round-oval-round roll drawing schedules were investigated (Ref 7). The effect of hydrodynamic and roller die drawing on the ferrite texture of low carbon steel wires were compared (Ref 8). The mechanical properties (tensile strength, yields strength, and percentage of elongation) of different steels which experienced roll drawing and cold rolling were compared (Ref 9). Bayoumi (Ref 10) has analyzed the deformation pattern in roll drawing process in round to square pass by developing an analytical solution for deformation of material.

In the present work, a three-dimensional simulation of roll drawing process to produce flat wires is developed. The influence of some process parameters on final profile of the flat wire is investigated (e.g., incoming wire diameter, forming rolls diameter, thickness reduction, and friction conditions). To examine the model predictions, roll drawing of a low carbon steel wire, with different diameters, is investigated and geometrical measurements of profile are performed on experimental samples. The comparison of experimental data with numerical results shows a reasonable agreement between the two sets of data, therefore proving the validity of the employed model.

## 2. Numerical Model

### 2.1 Formulation

Numerical simulation of wire drawing with roller dies is performed to investigate the deformation behavior of flat wire produced with such a process. In the simulation, an elastic-plastic material model is assumed whereas the stress and strain distributions satisfy the equilibrium equations, the constitutive equations and the prescribed boundary values such

F. Lambiase and A. Di Ilio, Department of Mechanical Energy and Management Engineering, University of L'Aquila, Monteluco di Roio, 67040 AQ, Italy. Contact e-mail: francesco.lambiase@univaq.it.

as symmetry, prescribed velocity and contacts. The workpiece obeys the Von-Mises yield criterion and Levi-Mises flow rule. As a quasi-static process is supposed, the body forces can be neglected and the equilibrium equations can be expressed as:

$$\int_v \bar{\sigma} \delta \dot{\epsilon} dV - \int_{S_F} F_i \delta u_i dS = 0, \quad (\text{Eq 1})$$

where  $\bar{\sigma}$  is the effective stress,  $\dot{\epsilon}$  is the effective strain rate, and  $F_i$  represents the traction forces on surface  $S_F$ . In addition,  $\delta u_i$  is the variation of an admissible velocity field  $u_i$  from which the variation of effective strain rate is calculated. To remove the incompressibility constraint on the admissible velocity fields, a penalty constant,  $K$ , may be used and Eq 1 becomes:

$$\int_v \bar{\sigma} \delta \dot{\epsilon} dV - K \int_v \dot{\epsilon}_v \delta \dot{\epsilon}_v dV - \int_{S_F} F_i \delta u_i dS = 0 \quad (\text{Eq 2})$$

## 2.2 Modeling

A 3-D FEM is developed to predict the final profile of wire. The wire geometry is meshed with tetrahedral eight-node linear bricks; moreover, to accurately account the final wire profile, the element dimension within the plane perpendicular to drawing direction ( $z$ -axis), was set to 0.2 mm. Such a value is preferred to better estimate the width of contact area between the wire and rolls,  $b$ . Indeed, a series of previous simulations was conducted to determine the optimal values of element size and it is carried out that although an element size of 0.3 mm in  $z$ -plane is small enough to accurately evaluate the lateral spreading of material, such a value is too big for an accurate evaluation of  $b$ -parameter. A coarser mesh size of 0.4 mm is used in drawing direction to reduce the computational time and also guarantee a sufficient number of elements along the contact arc between wire and roll, thus providing a good prediction of material flow within the plastic deformation zone. The simulations are run with and without meshing. As mentioned in previous section, the wire material is modeled as elastic-plastic and an isotropic deformation hardening is accounted for the plastic regime. The effects of strain rate and temperature can be retained negligible since the process is cold forging and the heat generated in the process is not sufficient to significantly modify the material properties, thus the process is assumed isothermal. Roll drawing experiments are carried out on a low carbon steel AISI 1010. Such a material is characterized by a good ductility and relative low yield stress. In order to evaluate the material characteristics in elastic and plastic regimes, tensile tests were performed on a 250 kN servo-hydraulic material testing machine according to ASTM E8M standard. The effective stress-strain curve is modeled with the power law given by Eq 1, whereas the static yield stress ( $\sigma_0 = 475$  MPa), the strain hardening index ( $n = 0.3$ ), and the strength coefficient ( $K = 650$  MPa) are determined by regression of tensile tests data.

$$\sigma = \sigma_0 + K \epsilon_p^n \quad (\text{Eq 3})$$

Also, the elastic modulus and Poisson ratio are 203 GPa and 0.3. As the drawing process with flat roller dies is symmetric about the  $z$ - $x$  and  $y$ - $z$  planes, only a quarter of the wire and rolls is simulated. The roller die is modeled as a cylindrical rigid surface with five degrees of freedom (DOF) constrained, while

the latter DOF, i.e., the rotation about the rolling axis, is unconstrained. A sliding-sticking friction model is used to reproduce the contact behavior of troll-wire interface. The frictional stress follows Tresca's law above the shear yield stress of the material  $\tau_y = m\sigma_y/\sqrt{3}$ , where  $m$  and  $\sigma_y$  are the friction coefficient and the normal yield stress, respectively. Over such a value, the friction becomes sticking and does not depend on the compressive normal stress. Because of the AISI 1010 is characterized by a moderate slope of flow stress with plastic deformation, confirmed by a small value of the strain hardening index  $n$ , a constant value of  $\sigma_y$  is assumed for the computation of shear yield stress which regulates the transition from sliding to sticking mode of friction. Because of the process is cold forming, different coefficients of frictions in range from 0.02 to 0.15 are tested. A friction coefficient of 0.1 is subsequently used in further simulations since it provides the best fit with experimental measurements.

## 2.3 Experimental Apparatus and Tests

A flexible prototypal apparatus is employed to conduct the experimental tests. The employment of moving cursors, on which the working rolls are mounted, allows conducting experimental tests with different thickness reduction, i.e., by changing the forming rolls diameter and/or the rolls clearance, as shown in Fig. 1. The desired final height of wire can be achieved by the adoption of a given number of calibrated blocks. The experimental tests are conducted wires with different diameters 5.4 and 4.6 mm. A number of thickness reductions are tested ranging between 10 and 60%, since over 60% of thickness reduction the breaking of wire occurred. The thickness reduction refers to the theoretical reduction, as usual Eq 4:

$$r = \frac{d_0 - t}{d_0}, \quad (\text{Eq 4})$$

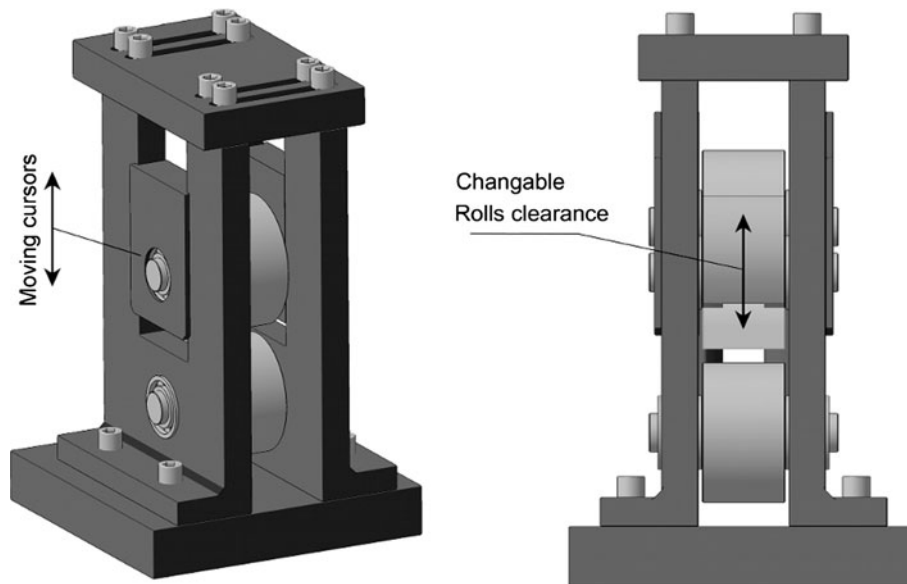
where  $d_0$  is the initial wire diameter and  $t$  is the height of flat wire. At each deformation condition the geometrical characteristics, i.e., final width, final height, and the width of contact area, are measured by means of an optical microscope.

## 3. Results and Discussion

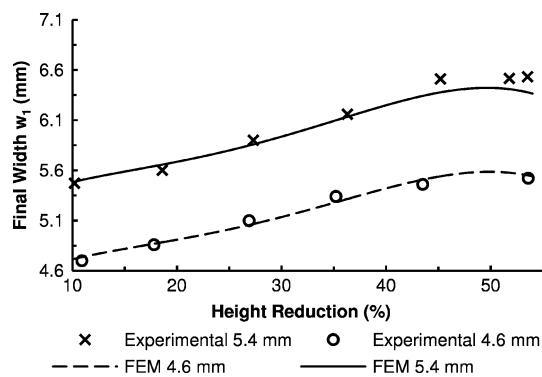
In this section, the effects of various process parameters such as initial wire diameter, rolls diameter, thickness reduction, and friction conditions are investigated using experimental measurements and 3-D numerical model of roll drawing process.

### 3.1 Validation of Numerical Model

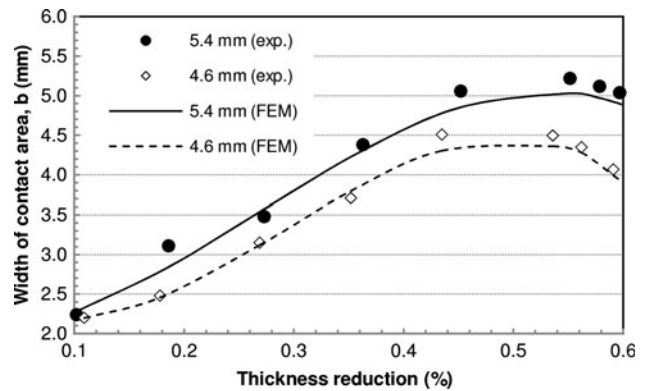
Before presenting the results of FE model, it is important to analyze the accuracy of the numerical model. The model validation is performed by comparing the final geometry of flat wires achieved during experimental tests, at different process conditions, with the numerical counterpart, in terms of final width of wire and width of contact area between wire and rolls. In Fig. 2, the experimental measurements of final width of wire at different thickness reductions and the corresponding numerical values calculated with the FEM are shown. FE results are in good agreement with experimental data throughout the entire analyzed range. Indeed, the maximum error is lower than 2%.



**Fig. 1** Schematic representation of the experimental machine used in roll drawing tests



**Fig. 2** Comparison between experimental measurements of final wire width and corresponding model results at different height reductions, with forming rolls diameter  $D = 80$  mm, for different wire diameters



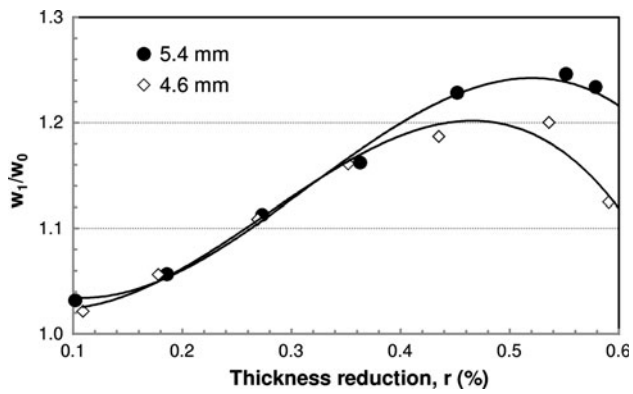
**Fig. 3** Comparison between experimental measurements of width of contact area,  $b$ , and corresponding model results, while using forming rolls of diameter  $D = 80$  mm, at different height reductions for different wire diameters

Figure 3 depicts the trend of the width of contact area between the wire and the rolls,  $b$ , obtained by experimental measurements and numerical model. Also considering this characteristic, a good agreement between FE model and experimental findings is observed. Therefore, it can be concluded that the developed FEM of roll drawing can be used to evaluate and predict the geometrical characteristics of flat wire.

The results of 3-D modeling are presented as follows. For medium deformations the element distortion is relatively small therefore proving the accuracy of model even without using adaptive meshing techniques. Indeed, below thickness reduction of 50%, any significant difference was found among results provided by simulations with and without adaptive meshing; conversely, at higher thickness reductions, from 50 to 60% adaptive meshing allowed to better predict the material flow. Actually, over certain values of thickness reduction (depending on the wire and rolls diameter), necking occurs on the final section of wire; therefore, the element distortion caused by the severe deformation does not allow simulations without adaptive meshing to converge and complete.

### 3.2 Thickness Reduction

In Fig. 4, the variation of lateral spread of wire, calculated as  $w_1/w_0$ , with the thickness reduction on wires of different diameters, i.e., 5.4 and 4.6 mm, are presented. It can be observed that, at small height reductions, the lateral spread of wire increases with the increase of height reduction for both wire diameters. However, as the wire undergoes more severe thickness reductions, the lateral spread exhibits a maximum, than decreases. A further increase of thickness reduction  $r = 60\%$ , usually determines the wire breakage due to excessive tensile stress acting at the exit section of wire. Comparing the behavior shown by different wire diameter, it can be observed that at small and medium values of thickness reduction ( $r < 0.4$ ), the lateral spread of wire is almost identical for two wire diameters. On the other hand, for more severe thickness reductions, the larger the wire initial diameter, the larger the lateral spread. This characteristic may not be addressed to the length of contact arc. In order to verify such hypothesis, the trend of the length of contact arc,  $L$ , is depicted



**Fig. 4** Variation of lateral spread of wire with the reduction thickness using forming rolls of diameter  $D = 80$  mm, for various wire diameters

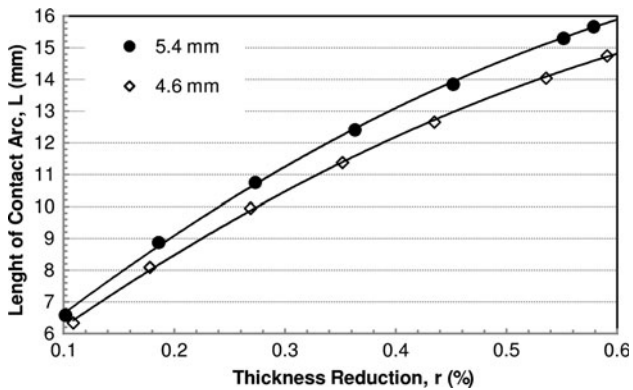


**Fig. 5** Variation of length of contact arc with thickness reduction for different wire diameters and forming rolls diameter  $D = 80$  mm

versus the thickness reduction,  $r$ . As usually done for rolling process, whether the ratio of rolls diameter,  $D$ , by initial wire diameter  $w_0$  is sufficiently high,  $L$  can be approximated by Eq 5:

$$L = \sqrt{R \cdot \Delta h} \quad (\text{Eq 5})$$

As evident from Fig. 5, the trends of  $L$ -values versus thickness reduction of different wires are very similar along the overall range of thickness reduction and would not explain the sudden difference of lateral spread occurring at medium-high values of thickness reduction. On the other hand, a qualitative reason of such a difference, would address the sudden decrease of lateral spread of wire to the occurrence of high tensile stress in axial direction which cause a partial contraction in lateral direction, similarly to necking phenomenon during tensile tests.

Figure 6 depicts the trend of width of contact area  $b$ , versus the length of contact area,  $L$ . It can be seen that for small-medium values of thickness reduction, to which corresponds a value of  $L$  in range: 6-13 mm, the trend of  $b$  is almost linear with  $L$  and only negligible difference exists between wires of diameter 5.4 and 4.6, thus proving the strong linear correlation between  $b$  and  $L$ , as in rolling of slabs. Conversely, at higher values of thickness reduction, the trend of  $b$  shows a gentle decrease due necking occurrence. In addition, the trend of width of contact area depicted in Fig. 6 suggests that in smaller wire, i.e., 4.6 mm of diameter, necking phenomenon occurs at

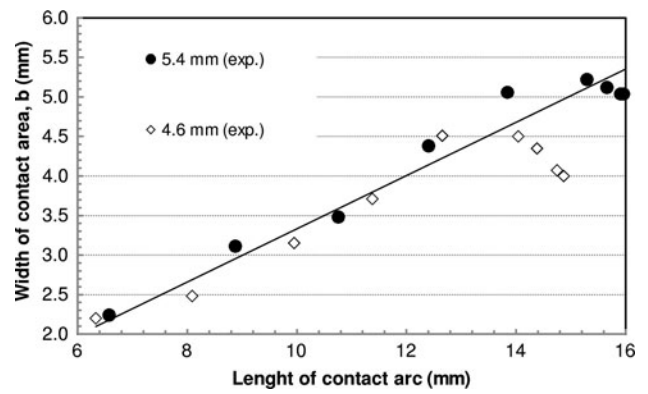


**Fig. 6** Variation of width of contact area with length of contact arc for different wire diameters

lower values of thickness reduction with respect to larger one. Also in this case, it can be observed that the influence of arc of contact length between wire and rolls can be retained negligible for small thickness reduction, while conversely it determines the occurrence of wire necking at more severe thickness reductions.

### 3.3 Rolls Diameter

To investigate the effects of arc of contact length and forming roll diameter on final geometry of flat wire, a number of experiments and simulations are conducted by changing the rolls diameter in range 40-120 mm on both wires (5.4 and 4.6 diameters). As the two wires are characterized by similar behaviors, following only the results concerning the wire with diameter 5.4 mm are reported, since analogous considerations can be turned out for wire of diameter 4.6. Figure 7 shows the variation of lateral spread of wire with forming rolls diameter at different values of thickness reduction,  $r$ . As can be noted, an increase of roll diameter determines an increase of lateral spread of wire in the overall range of analyzed thickness reductions. In small-medium range of thickness reduction, the lateral spread is more sensitive to thickness reduction with respect to forming rolls diameter. Conversely, for more severe deformations, the forming rolls diameter effect is predominant of lateral spread with respect to thickness reduction. Indeed, a negligible difference can be observed between the lateral spread at  $r = 0.4$  and  $r = 0.5$  aside forming rolls diameter, as can be also observed in Fig. 4. In addition, the effect of rolls diameter is more prominent at higher values of thickness reduction (the slope of curves increases from  $r = 0.1$  to  $r = 0.5$ ).

Data in Fig. 7 are rearranged to further investigate the influence of forming rolls on lateral spreading of wire as depicted in Fig. 8. As can be seen, the trend of lateral spread at small-medium thickness reductions, i.e.,  $r < 0.4$ , is almost linear with length of contact arc,  $L$  (and consequently with thickness reduction) for all forming rolls diameters, i.e., 40, 80, and 120 mm.

### 3.4 Friction Conditions at Wire-Roll Interface

A number of experiments are carried out by changing both the thickness reduction and the lubrication conditions at wire-rolls interface. A series of simulations is conducted by varying the friction coefficient  $m$  from 0.02 to 0.15. Figure 9 depicts the experimental measurements (with and without lubrication) and



numerical predictions (with different friction coefficients, i.e., 0.02, 0.1, and 0.15) of lateral spread achieved at different thickness reductions. As it can be observed the effect of lubrication on geometrical characteristics of flat wires is almost negligible. Conversely, the FE model results suggest a certain dependence of lateral spread and width of contact area on the friction conditions arising at wire-roll interface. Although the

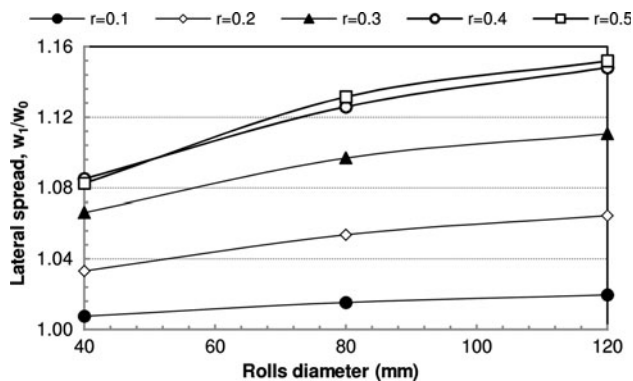


**Fig. 7** Variation of lateral spread of wire with roll diameter on wire  $w_0 = 5.4$  mm at different thickness reductions

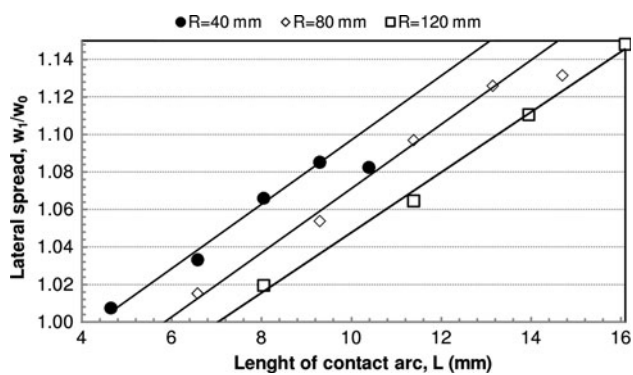


**Fig. 8** Variation of width of contact area with length of contact arc on wire  $w_0 = 5.4$  mm with different working rolls diameter

effect of thickness reduction is predominant as compared to lubrication conditions, the simulation results suggest a minor but not negligible effect of friction on lateral spread, and particularly the higher the friction coefficient the higher the lateral spread of material. This discrepancy between experimental measurements and numerical results can be addressed to the distribution of contact pressure between the wire and rolls. Indeed, similarly to flat rolling process (Ref 2), the stress rise in the roll entry zone and the edge surrounding the contact zone, shown in Fig 10, can reduce or even avoid the penetration of lubricant between the rolls and wire in the plastic deformation zone.

#### 4. Conclusions

In this work, a prototypal apparatus is used to perform experimental tests on the wire drawing process using flat idle rolls. The effects of various process parameters such as thickness reduction, wire diameter, lubrication conditions, and

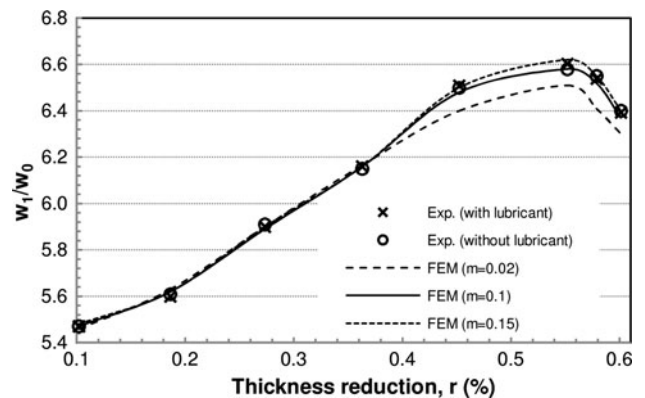


**Fig. 9** Effect of lubrication conditions on lateral spread and width of contact area at wire-rolls interface at different thickness reduction and working rolls diameter of 80 mm as measured on experimental samples and calculated with numerical model at different friction coefficients 0.02, 0.1, and 0.15

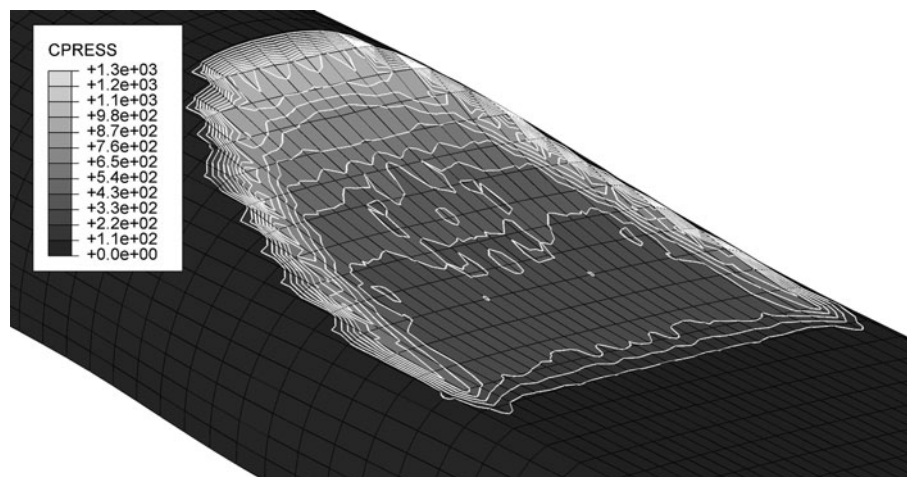


**Fig. 10** Representative distribution of contact pressure at rolls-wire interface (thickness reduction  $r = 0.5$ , initial wire diameter  $w_0 = 5.4$  mm, and forming rolls diameter  $D = 80$  mm)

forming rolls diameter on final geometry of flat wire are estimated by analyzing both experimental measurements and numerical results. Initially, the numerical model is validated by varying the process parameters among several levels and comparing the main geometrical characteristics of flat wires, namely the width and width of contact area between rolls and wire measured experimentally and calculated by FE model. The most important results are summarized as follows:

- The 3D FEM was capable to predict with good precision the final profile of wire: the maximum error in evaluation of final width is 2%.
- The adoption of adaptive meshing is not required for values of thickness reduction smaller than 0.5 while on the other than it dramatically improves the results accuracy for more severe reductions due to necking occurrence.
- The thickness reduction is characterized by three different range, namely, small-medium reduction ( $r < 0.4$ ), severe reduction ( $0.4 < r < 0.5$ ), and necking range ( $r > 0.5$ ). At small-medium range, the lateral spread is almost linear with variation of thickness reduction. Within severe reduction range, the spread is not significantly influenced by thickness reduction and conversely at necking range the higher the thickness reduction the smaller the lateral spreading of wire.
- Within the small-medium reduction range, lateral spreading of wire is principally influenced by thickness reduction; conversely, forming rolls diameter has a small influence on lateral spread. In addition, for thickness reduction smaller than 0.35 the initial wire diameter influence on lateral spread can be retained negligible.
- Within the severe reduction range, lateral spreading of wire is mostly influenced by the forming rolls diameter while, on the other hand, the thickness reduction has a negligible effect. Further, the smaller wire (4.6 in diameter) is characterized by an earlier necking phenomena with respect to larger wire (5.4 mm in diameter).

- Both lateral spread and width of contact area show a linear trend with respect to length of contact arc for values of thickness reduction smaller than 0.4.
- Final wire geometry is essentially independent on the friction condition. This may be originated by the rise at the entry zone and at the edges of contact zone of contact stress which may inhibit the penetration of lubricant at wire-roll contact interface.

## References

1. B. Carlsson and J. Lagergren, The Deformation of Drawn Wire in Flat Rolling, *Proc. ESDA 96, Third Biennial Joint Conf. on Eng. Syst. Design and Analysis*, Vol 3, ASME, New York, 1996, p 175–180
2. B. Carlsson, The Contact Pressure Distribution in Flat Rolling of Wire, *J. Mater. Process. Technol.*, 1998, **73**, p 1–6
3. M. Kazeminezhad and A. Karimi Taheri, A Theoretical and Experimental Investigation on Wire Flat Rolling Process Using Deformation Pattern, *J. Mater. Des.*, 2005, **26**, p 99–103
4. M. Kazeminezhad and A. Karimi Taheri, The Prediction of Macroscopic Shear Bands in Flat Rolled Wire Using the Finite and Slab Element Method, *Mater. Lett.*, 2006, **60**, p 3265–3268
5. M. Kazeminezhad and A. Karimi Taheri, Deformation Inhomogeneity in Flattened Copper Wire, *J. Mater. Des.*, 2007, **28**, p 2047–2053
6. C. Vallellano, P.A. Cabanillas, and F.J. Garcia-Lomas, Analysis of Deformations and Stresses in Flat Rolling of Wire, *J. Mater. Process. Technol.*, 2008, **195**, p 63–71
7. J.W. Pilarczyk, H. Dyja, B. Golis, and E. Tabuda, Effect of Roller Dies Drawing on Structure, Texture and Other Properties of High Carbon Steel Wires, *Met. Mater.*, 1998, **4**, p 727–731
8. J.W. Pilarczyk, P. Van Houtte, and E. Aernoudt, Effect of Hydrodynamic and Roller Die Drawing on the Texture of High Carbon Steel Wires, *Int. J. Mater. Sci. Eng. A*, 1995, **197**, p 97–101
9. J. Luksza and M. Burdek, The Influence of the Deformation Mode on the Final Mechanical Properties of Products in Multi-Pass Drawing and Flat Rolling, *J. Mater. Process. Technol.*, 2002, **125–126**, p 725–730
10. L.S. Bayoumi, Round-to-Square Section Drawing Through Flat Idle Rolls, *Int. J. Mech. Sci.*, 1999, **41**, p 1323–1338